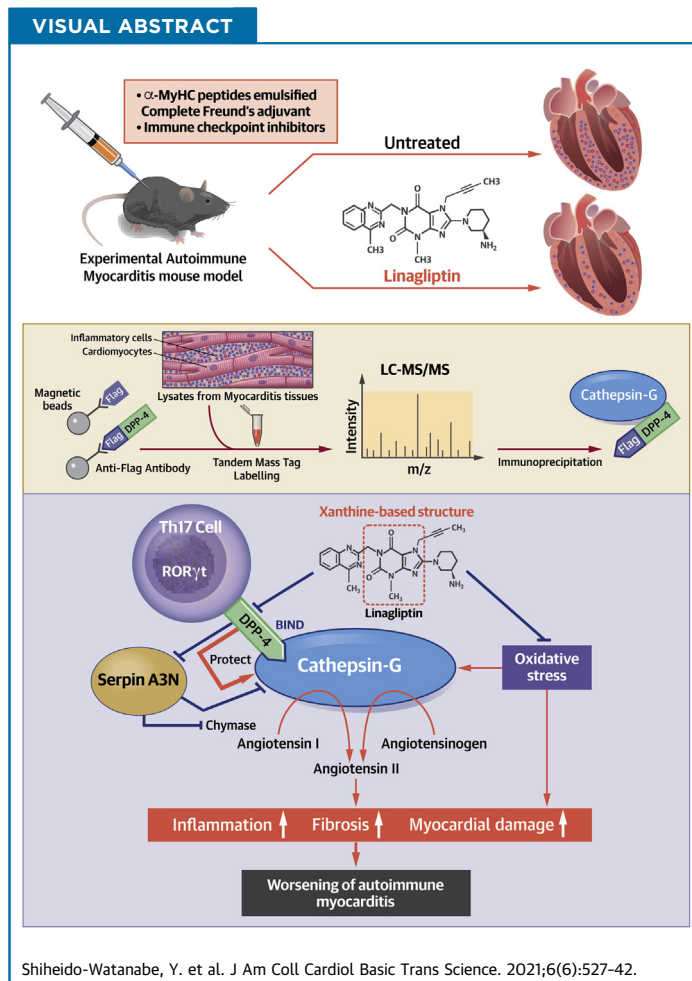


PRECLINICAL RESEARCH

# Linagliptin, A Xanthine-Based Dipeptidyl Peptidase-4 Inhibitor, Ameliorates Experimental Autoimmune Myocarditis



Yuka Shiheido-Watanabe, DDS, PhD,<sup>a</sup> Yasuhiro Maejima, MD, PhD,<sup>a</sup> Takeshi Kasama, PhD,<sup>b</sup> Natsuko Tamura, MD, PhD,<sup>a</sup> Shun Nakagama, MD,<sup>a</sup> Yusuke Ito, MD, PhD,<sup>a</sup> Kenzo Hirao, MD, PhD,<sup>a,c</sup> Mitsuaki Isobe, MD,<sup>a,d</sup> Tetsuo Sasano, MD, PhD<sup>a</sup>



**HIGHLIGHTS**

- Treatment with linagliptin, a DPP-4 inhibitor, alleviates not only EAM but also ICIM.
- DPP-4 physically interacts with cathepsin G and enhances its activity.
- Linagliptin promotes SerpinA3N activity, thereby suppressing cathepsin G activity.
- Cathepsin G aggravates EAM through upregulating angiotensin II.
- Linagliptin suppresses oxidative stress in EAM hearts.

ABBREVIATIONS  
AND ACRONYMS**DPP** = dipeptidyl peptidase**EAM** = experimental  
autoimmune myocarditis**ELISA** = enzyme-linked  
immunosorbent assay**ICIM** = immune checkpoint  
inhibitor-induced myocarditis**LVDD** = left ventricular end-  
diastolic dimension**OHdG** = hydroxyguanosine**ROR $\gamma$ t** = RAR-related orphan  
nuclear receptor gamma**TMT** = tandem mass tag

## SUMMARY

This study sought to show the mechanism of how to ameliorate experimental autoimmune myocarditis (EAM) by administering dipeptidyl peptidase (DPP)-4 inhibitor linagliptin. The number of RAR-related orphan nuclear receptor gamma-positive Th17 cells infiltrated to the EAM myocardium was significantly attenuated by linagliptin treatment. Tandem mass spectrometry-based analysis demonstrated that DPP-4 binds to cathepsin G in EAM hearts, thereby protecting cathepsin G activity through inhibiting SerpinA3N activity. Linagliptin suppresses oxidative stress in EAM hearts as well. Thus, we found that DPP-4 plays a detrimental role in the progression of EAM by interacting with cathepsin G, which, in turn, suppresses SerpinA3N activity. (J Am Coll Cardiol Basic Trans Science 2021;6:527-42) © 2021 The Authors. Published by Elsevier on behalf of the American College of Cardiology Foundation. This is an open access article under the CC BY-NC-ND license (<http://creativecommons.org/licenses/by-nc-nd/4.0/>).

Myocarditis is the leading cause of nonhereditary heart failure developing at a young age (<40 years old) (1). Among patients with myocarditis who were diagnosed by histologic evidence with a myocardial biopsy, 10% to 20% of patients will develop to dilated cardiomyopathy (2). The frequency of autoimmunity-mediated myocarditis is relatively low compared with that of infection-mediated myocarditis. However, it is important to identify the cause of myocarditis to choose effective therapeutic strategies including immunosuppressive therapy. Additionally, recently, autoimmune myocarditis was identified as a serious side effect of immune checkpoint inhibitors, a novel category of anticancer drugs that help direct the immune system to recognize and target cancer cells (3,4). Thus, it is imperative to identify mechanisms leading to myocarditis based on autoimmune abnormalities and develop effective therapies.

Dipeptidyl peptidase (DPP)-4 is a membrane glycoprotein of 110 kDa and a serine protease that cleaves X-proline/alanine dipeptides from the N-terminus of polypeptides. The most well-known substrates of DPP-4 are incretins such as glucagon-like peptide-1 and glucose-dependent insulintropic polypeptide. When DPP-4 is inhibited, blood levels of incretins are raised and act on both pancreatic islet cell types, thereby promoting hypoglycemic action in those cells. Currently, DPP-4 inhibitors are the most

widely used drugs in the treatment of diabetes because of their efficacy and safety for low-incidence hypoglycemia. On the other hand, increasing lines of evidence suggest that DPP-4 is critical for the regulation of inflammatory responses (5).

DPP-4, also known as CD26, is expressed on the cell surface of T lymphocytes and acts as a costimulatory pathway of T lymphocytes; this pathway is involved in the regulation of the cell-mediated immune system (6). Bengsch et al. (7) demonstrated that an active form of CD26 is highly expressed on the cell surface of Th17 lymphocytes, a subtype of helper T lymphocytes that are considered to be involved in the pathogenesis of autoimmune diseases. In addition, Zhong et al. (8) demonstrated that CD26 on dendritic cells/macrophages plays a critical role in promoting obesity-induced visceral inflammation. These findings led us to hypothesize that the inhibition of DPP-4 could be effective for the suppression of autoimmune myocarditis. We have previously demonstrated that linagliptin, a selective DPP-4 inhibitor that has a high degree of affinity for DPP-4 in various tissues (9-11), is useful in an experimental autoimmune myocarditis (EAM) model (12). However, the precise mechanism through which linagliptin exerts its anti-inflammatory effect to suppress myocarditis remains to be elucidated.

In this study, we demonstrated that DPP-4 physically interacts with cathepsin G, a plasma membrane-bound serine protease, in EAM mice

From the <sup>a</sup>Department of Cardiovascular Medicine, Tokyo Medical and Dental University, Tokyo, Japan; <sup>b</sup>Research Center for Medical and Dental Sciences, Tokyo Medical Dental University, Tokyo, Japan; <sup>c</sup>Department of Cardiovascular Medicine, AOI Universal Hospital, Kawasaki City, Japan; and the <sup>d</sup>Sakakibara Heart Institute, Japan Research Promotion Society for Cardiovascular Diseases, Tokyo, Japan.

The authors attest they are in compliance with human studies committees and animal welfare regulations of the authors' institutions and Food and Drug Administration guidelines, including patient consent where appropriate. For more information, visit the [Author Center](#).

Manuscript received February 16, 2021; revised manuscript received April 8, 2021, accepted April 27, 2021.

hearts. Furthermore, we also present evidence suggesting that the suppression of cathepsin G activity by the administration of linagliptin effectively attenuates myocardial inflammation by regulating the activities of both SerpinA3N and angiotensin II in EAM mice.

## METHODS

### EXPERIMENTAL ANIMAL MODELS OF MYOCARDITIS.

Male BALB/c mice (6 weeks of age, body weight: 20–25 g) were purchased from Japan Clea, Co. (Tokyo, Japan). All animal care and experimental procedures were approved by the Tokyo Medical and Dental University Guide for the Care and Use of Laboratory Animals (permit number: A2018-184A) and by the Guide for the Care and Use of Laboratory Animals published by the US National Institutes of Health.

Experimental autoimmune myocarditis was induced in BALB/c mice by subcutaneous injection of the  $\alpha$ -myosin heavy chain peptides (150  $\mu$ g per mouse) emulsified with complete Freund's adjuvant on days 0 and 7. On day 0, 500 ng pertussis toxin was also administered intraperitoneally at the same time to induce the EAM mice model. EAM mice were assigned to 1 of the following 2 groups: the EAM mice group treated with linagliptin (3 mg/kg) and untreated controls. Mice were sacrificed on day 21. For the experiments of angiotensin II receptor type 1 blockade, losartan (10 mg/kg/day; Merck & Co., Inc., Kenilworth, New Jersey) was given to the mice in their drinking water (13).

To generate the immune checkpoint inhibitor-induced myocarditis (ICIM) model, the antimouse PD-1 monoclonal antibody (200  $\mu$ g per mouse [RMP1-14, Leinco Technologies, St. Louis, Missouri]), antimouse PD-L1 monoclonal antibody (150  $\mu$ g per mouse [10F.9G2, Leinco Technologies]), or their isotype control monoclonal antibodies (rat IgG2a or rat IgG2b) were intraperitoneally administered in male MRL/MpJ-*Fas*<sup>lpr</sup> mice (8 weeks of age, body weight: 25–30 g, Japan SLC, Hamamatsu, Japan) on the same days (days 0, 3, 7, 10, 14, 17, and 21). Mice were sacrificed on day 28.

**ECHOCARDIOGRAPHY.** Transthoracic echocardiography was performed on animals anesthetized by the intraperitoneal administration of 3.6% chloral hydrate (Wako Pure Chemical Industries, Osaka, Japan) in saline (0.1 ml/10 g body weight). For the left ventricular echocardiographic recording, an echocardiographic machine with a 14-MHz transducer (Toshiba, Tokyo, Japan) was used. A 2-dimensional targeted M-mode and B-mode echocardiogram was obtained along the short-axis view of the left

ventricle at the level of the papillary muscles. Left ventricular end-diastolic (LVDD) and end-systolic dimensions and left ventricular fractional shortening (left ventricular fractional shortening = [LVDD – left ventricular end-systolic dimension]/LVDD) were calculated from M-mode echocardiograms over 3 consecutive cardiac cycles according to the American Society for Echocardiography leading-edge method. The measurements of 3 consecutive cardiac cycles were averaged. Measurements were made off-line by 2 independent investigators.

**HISTOPATHOLOGY.** Hearts were harvested immediately after animals were sacrificed by cutting the abdominal aorta under deep anesthesia on day 21. After measuring the weight (mg), midventricular slices of the heart were stained with hematoxylin and eosin and Mallory methods. Blue staining of collagen fibers was quantified as a measure of fibrosis using the Image-Pro Express software program (Media Cybernetics, Rockville, Maryland). The area of the myocardium affected by cell infiltration was determined as infiltrated. All data were analyzed in a blind fashion by 2 independent investigators and averaged.

**IMMUNOHISTOCHEMISTRY.** Immunohistochemistry was performed to evaluate the amount of a thymus-specific isoform of the RAR-related orphan nuclear receptor gamma (ROR $\gamma$ t), cathepsin G, and 8-hydroxyguanosine (OHdG), a marker of oxidative stress in DNA, in the hearts of mice on day 21. Frozen sections were fixed in acetone at 4°C. The sections were incubated with unlabeled primary antibodies overnight at 4°C and washed in phosphate-buffered saline. The antibody-horseradish peroxidase conjugate was detected with a Histofine Simple Stain Kit (Nichirei Corporation, Tokyo, Japan) following the manufacturer's instructions. ROR $\gamma$ t-positive cells were counted, and the number was divided by the entire area.

**DPP-4 ACTIVITY ASSAY.** The activity of DPP-4 was evaluated in myocardium tissues using a DPP-4 activity assay kit (BioVision, Milpitas, California) according to the manufacturer's instructions.

**T-CELL PROLIFERATION ASSAY.** Spleen cells were isolated from mice with myocarditis on day 18. Cells ( $5 \times 10^5$ /well) were cultured in 96-well plates with 50  $\mu$ g/ml purified porcine heart myosin (Sigma-Aldrich, St. Louis, Missouri). Linagliptin was added to each well at various concentrations. Cells were incubated at 37°C under 5% CO<sub>2</sub> for 3 days. T-cell proliferation was assessed by the 3-(4,5-dimethylthiazol-2-yl)-2,5-diphenyltetrazolium bromide assay with the Cell Counting Kit-8 (Dojindo, Tokyo, Japan). Cell proliferation was expressed as the optical density (14).

**PROTEIN EXTRACTION FROM THE MYOCARDIUM.**

Heart specimens, which were harvested immediately after mice were sacrificed on day 21, were homogenized in radioimmunoprecipitation assay buffer (50 mmol/l Tris-HCl [pH = 7.6], 150 mmol/l NaCl, 0.5% deoxycholic acid, 0.1% sodium dodecyl sulfate, and 1% NP-40). Regarding the samples used for tandem mass tag (TMT) labeling, heart specimens were homogenized in a Minute Plasma Membrane Protein Isolation Kit (Invent Biotechnologies, Inc., Plymouth, Minnesota). Samples were centrifuged, and the supernatant was transferred to new tubes. Protein concentration was determined using a BCA protein assay (Pierce Biotechnology, Rockford, Illinois). Proteins were stored at  $-80^{\circ}\text{C}$  until further analysis.

**IMMUNOPRECIPITATION.** Human embryonic kidney 293 cells were cultured for 18 to 24 h to approximately 80% confluence in 10-cm plates and then transfected with 10 ng plasmid (Flag-DPP-4 or Flag-Empty) using FuGene6 (20  $\mu\text{l}$ , Roche, Basel, Switzerland) according to the manufacturer's instructions. After 48 h of transfection, cells were harvested and solubilized in a lysis buffer (50 mmol/l Tris-HCl [pH = 7.4], 1% Triton X-100, 150 mmol/l NaCl, 1 mmol/l phenylmethylsulfonyl fluoride, and 10  $\mu\text{g}/\text{ml}$  aprotinin). Total cell lysates (500  $\mu\text{g}$ ) were immunoprecipitated with Flag antibody-conjugated magnetic beads overnight at  $4^{\circ}\text{C}$ . Immunoprecipitates were washed several times with lysis buffer.

**TMT LABELING.** Immunoprecipitates with Flag antibody-conjugated magnetic beads (described previously) were incubated with heart lysates extracted with the Minute Plasma Membrane Protein Isolation Kit for 6 h at  $4^{\circ}\text{C}$ . Cells were washed with 500  $\mu\text{l}$  tris-buffered saline with tween 20 for 10 min at  $4^{\circ}\text{C}$  5 consecutive times. They were then added to the elution buffer (0.1 mol/l glycine with HCl) and neutralized with 1 mol/l Tris-HCl (pH = 9.0). TMT labeling was performed using TMT Mass Tagging Kits and Reagents (ThermoFisher Scientific, Waltham, Massachusetts) according to the manufacturer's instructions. The eluted proteins were adjusted to 100  $\mu\text{L}$  with 100 mmol/l triethylammonium bicarbonate; additionally, 5  $\mu\text{l}$  of the 200 mmol/l tris(2-carboxyethyl)phosphine were added, and samples were incubated at  $55^{\circ}\text{C}$  for 1 h. Then, 5  $\mu\text{l}$  375 mmol/l iodoacetamide was added to the sample and incubated for 30 min protected from light at room temperature. Trypsin was added (final concentration: 2.5%) to sample proteins in triethylammonium bicarbonate, and samples were digested overnight at  $37^{\circ}\text{C}$ . As a labeling step, 41  $\mu\text{l}$  TMT label reagent (ThermoFisher Scientific) was added to each 100- $\mu\text{l}$

sample. After incubating the reaction for 1 h at room temperature, 8  $\mu\text{l}$  5% hydroxylamine was added to the sample and incubated for 15 min to quench the reaction.

**LIQUID CHROMATOGRAPHY WITH TANDEM MASS SPECTROMETRY ANALYSIS.**

The aliquot of TMT-labeled samples was analyzed using a LTQ Orbitrap Velos hybrid mass spectrometer (ThermoFisher Scientific) equipped with an Easy nLC II nano-LC system (Proxeon, Odense, Denmark) and Chip-Mate nano-ESI interface unit (Advion Inc., Ithaca, New York). The Nano-LC column was a MonoCap C18 Nano-flow 100  $\mu\text{m}$  i.d.  $\times$  750 mm (GL Sciences, Torrance, California). The nano-liquid chromatography settings were configured as follows: the flow rate was 300 nl/min, water containing 0.1% formic acid was used as eluent A, and acetonitrile/water (7:3, v/v) containing 0.1% formic acid was used as eluent B. The gradient of eluent B was set as follows: 0%, 5 min; 20%, 45 min; and 57%, 10 min. The acquired mass spectrometry and tandem mass spectrometry spectra were processed with Proteome Discoverer 1.3 Software (ThermoFisher Scientific).

**CATHEPSIN G ACTIVITY ASSAY.** The activity of cathepsin G was evaluated in myocardium tissues and mixtures of recombinant mouse DPP-4 (R&D Systems, Minneapolis, Minnesota), recombinant mouse SerpinA3N (R&D Systems), and cathepsin G (Enzo Biochem, New York, New York) using a cathepsin G Activity Assay Kit (Abcam, Cambridge, United Kingdom) according to the manufacturer's instructions. Briefly, the mixture of DPP-4, SerpinA3N, and cathepsin G or the mixture of SerpinA3N and cathepsin G was mixed with assay buffer and incubated at  $37^{\circ}\text{C}$  for 10 min. Then, the substrate solution (assay buffer and *p*-NA) was added to each well. Absorbance was detected at 405 nm using a microplate reader (Bio-Rad Laboratories, Hercules, California) at 0 min. A second read was performed after incubating the reaction at  $37^{\circ}\text{C}$  for 60 min protected from light.

**SerpinA3N ACTIVITY ASSAY.** The activity of SerpinA3N was evaluated in mixtures of DPP-4 and SerpinA3N and extracted proteins from the myocardium according to the manufacturer's instructions. The activity of SerpinA3N was measured by its ability to inhibit Granzyme B cleavage of *tert*-butoxycarbonyl-Ala-Ala-Asp-thiobenzyl ester (Boc-AAD-SBzl). Briefly, the mixture of DPP-4, SerpinA3N, and activated recombinant human Granzyme B (R&D Systems) or the mixture of SerpinA3N and Granzyme B was mixed with the assay buffer (50 mmol/l Tris, pH = 7.5). Then, the substrate mixture, which consisted of 5,5'-dithio-bis 2-nitrobenzoic acid

(Sigma-Aldrich), Boc-AAD-SBzl (SM Biochemicals, Anaheim, California), and assay buffer, was added to each well. The absorbance was detected at 405 nm in the kinetic mode for 5 min using a microplate reader (Bio-Rad Laboratories).

**ENZYME-LINKED IMMUNOSORBENT ASSAY.** The levels of SerpinA3N in homogenates of EAM hearts were determined by an enzyme-linked immunosorbent assay (ELISA) using an immunoassay kit (Aviva Systems Biology, San Diego, California). The ELISA was performed according to the manufacturer's instructions.

**ANGIOTENSIN II ASSAY.** The amount of angiotensin II was evaluated in myocardium tissues using an Angiotensin II ELISA kit (Sigma-Aldrich) according to the manufacturer's instructions.

**CHYMASE ACTIVITY ASSAY.** Chymase activity was measured as described previously (15). Briefly, tissue extracts were incubated for 30 min at 37°C with a substrate Suc-Ala-Ala-Pro-Phe-4-methylcoumaryl-7-amide (5 mmol/l; Fuji Film-Wako, Tokyo, Japan) in 100 mmol/l Tris-HCl buffer (pH = 8.5, 200 mmol/l NaCl). After termination of the enzyme reaction by adding 3% metaphosphoric acid (w/v), the amount of 7-amino-4-methylcoumarin was measured by fluorophotometric determination (excitation, 380 nm; emission, 460 nm). One unit of chymase activity was defined as the amount of enzyme that cleaved 1 μmol 7-amino-4-methylcoumarin/min.

**HYDROGEN PEROXIDE ASSAY.** EAM heart tissues (day 21) were homogenized and sonicated in 50 mmol/l potassium phosphate buffer and 0.5% hexadecyltrimethylammonium bromide. Samples were centrifuged, and the supernatant was transferred to new tubes. The concentration of hydrogen peroxide was determined using a hydrogen peroxide colorimetric/fluorometric assay kit (BioVision) according to the manufacturer's instructions.

**STATISTICS.** All statistical analyses were performed using PRISM version 8 (GraphPad Software, San Diego, California). All data are expressed as mean ± standard error of the mean. All statistical analyses were performed using an unpaired Student's *t*-test or 1-way analysis of variance followed by a post hoc Bonferroni-Dunn test for multiple pair-wise comparisons. A *p* value <0.05 was considered statistically significant.

## RESULTS

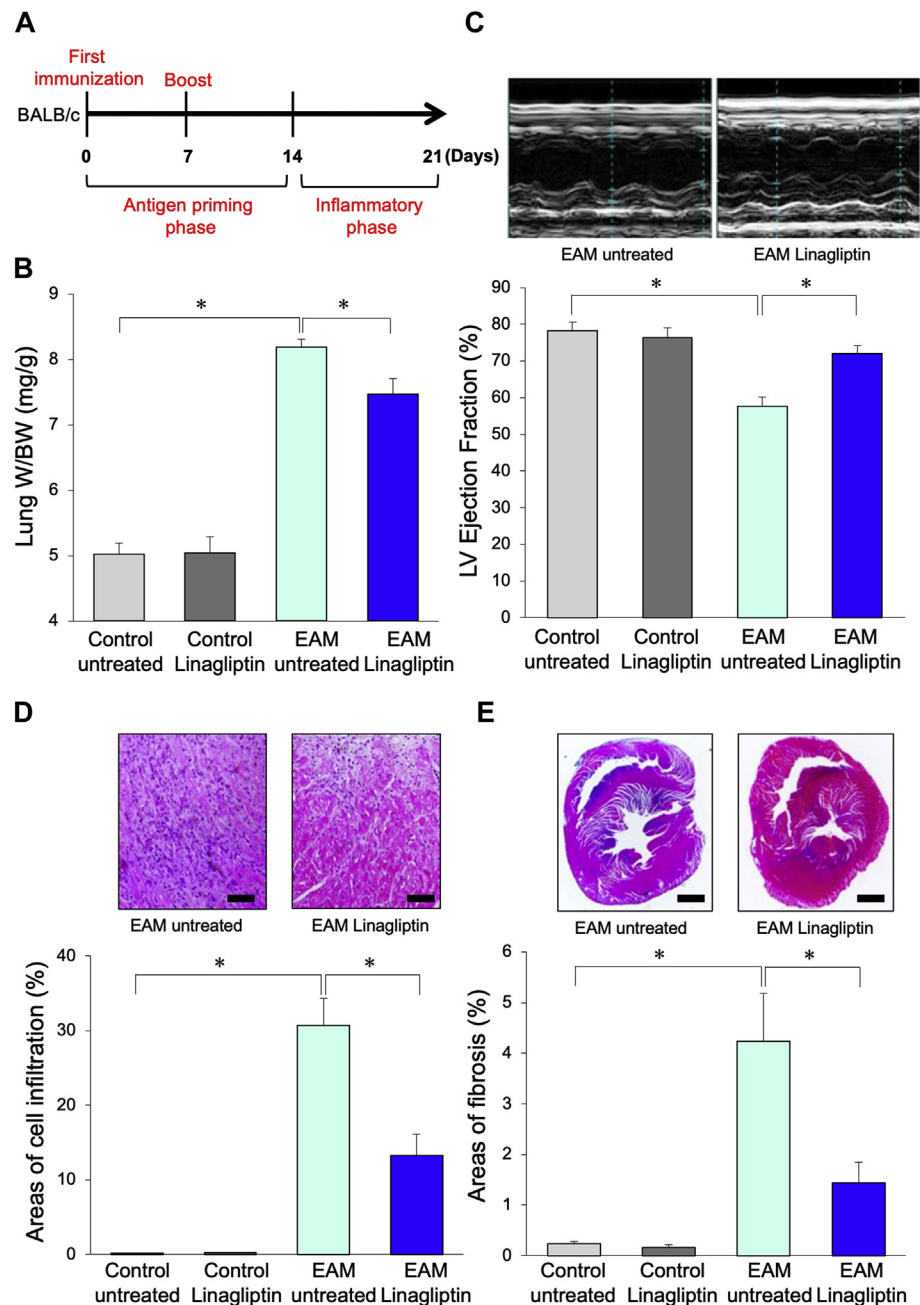
**TREATMENT WITH LINAGLIPTIN ATTENUATES PATHOLOGICAL PHENOTYPES OF EAM HEARTS.** We evaluated the effect of linagliptin on EAM mice

induced by immunizing with α-MyHC peptides (Figure 1A). Left ventricular systolic function, evaluated by echocardiographic examination, was significantly higher in linagliptin-treated EAM hearts than in untreated ones after 21 days of EAM induction (Figure 1B). The lung weight of linagliptin-treated EAM mice was significantly less than that of untreated ones (Figure 1C). Histopathologic examination revealed that inflammatory cell infiltration in EAM hearts was markedly attenuated by treatment with linagliptin after 21 days of EAM induction (Figure 1D); likewise, cardiac fibrosis after EAM induction was significantly decreased by treatment with linagliptin (Figure 1E). Taken together, these results suggest that linagliptin treatment effectively attenuates inflammatory cell infiltration and fibrosis in EAM hearts, thereby restoring cardiac dysfunction caused by EAM.

**TREATMENT WITH LINAGLIPTIN ALLEVIATES PATHOLOGICAL PHENOTYPES OF ICIM HEARTS.** We next evaluated the effect of linagliptin on ICIM mice induced by concurrent administration of both anti-mouse PD-1 monoclonal antibody and anti-mouse PD-L1 monoclonal antibody (Figure 2A). Histopathologic examination revealed that inflammatory cell infiltration in EAM hearts was markedly attenuated by treatment with linagliptin after 28 days of ICIM induction (Figures 2B and 2E). Left ventricular systolic function was significantly higher in linagliptin-treated ICIM hearts than in untreated ones after 28 days of ICIM induction (Figure 2D). Furthermore, the lung weight and myocardial fibrotic area of linagliptin-treated ICIM mice was significantly less than that of untreated ones (Figures 2C and 2F). These results suggest that linagliptin treatment effectively attenuates inflammatory cell infiltration in ICIM hearts, thereby restoring cardiac dysfunction caused by ICIM.

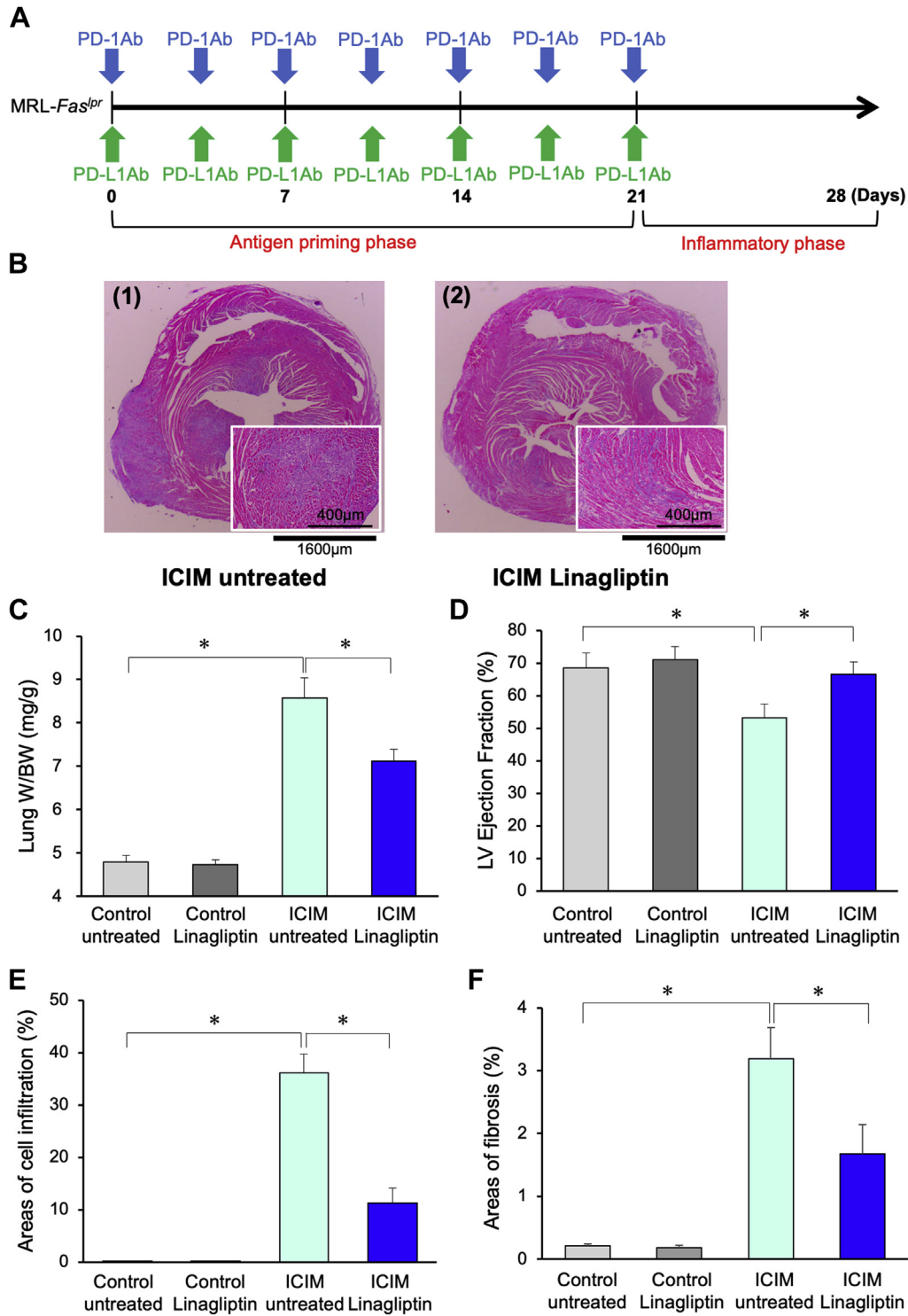
**THE INCREASE IN DPP-4 ACTIVITY WAS SIGNIFICANTLY SUPPRESSED BY LINAGLIPTIN TREATMENT IN EAM HEARTS.** We then elucidated the mechanism through which DPP-4 aggravates EAM. The activity of DPP-4 in EAM myocardial tissues was significantly elevated compared with those in control mice, and its activity was significantly suppressed by linagliptin treatment (Figure 3A). Increasing lines of evidence suggest that EAM is transferable to other individuals via EAM-derived splenic T cells (16). To examine the effect of linagliptin on antigen-induced T-cell proliferation, we conducted T-cell proliferation assay using EAM-derived splenocytes and found that treatment with linagliptin suppressed myosin-induced T-cell proliferation in a dose-dependent manner (Figure 3B).

It has been shown that Th17 cells express high levels of enzymatically active DPP-4 and enhance the

**FIGURE 1** Treatment With Linagliptin Attenuates Inflammatory Cell Infiltration and Fibrosis in EAM Hearts

**(A)** A schematic of the experimental design for experimental autoimmune myocarditis (EAM). BALB/c mice were subcutaneously injected with  $\alpha$ -myosin heavy chain peptides emulsified with complete Freund's adjuvant on days 0 and 7 with or without linagliptin administration. Mice were sacrificed for analyses on day 21. **(B)** Representative M-mode echocardiograms and quantitative analyses of left ventricular ejection fraction in EAM mice and EAM mice administered linagliptin. \* $p < 0.05$ ,  $n = 6$ . Data are expressed as mean  $\pm$  standard error of the mean (SEM). **(C)** The lung weight to body weight ratio in EAM mice and EAM mice administered linagliptin. \* $p < 0.05$ ,  $n = 6$ . Data are expressed as mean  $\pm$  SEM. **(D)** The representative results of inflammatory cell infiltration and quantitative analysis of the cell infiltration area in the myocardium of EAM mice and EAM mice administered linagliptin. Scale bar: 100  $\mu$ m, \* $p < 0.05$ ,  $n = 6$ . Data are expressed as mean  $\pm$  SEM. **(E)** Representative pathological images with Mallory staining in a low-power microscopic field and quantitative analysis of the fibrotic area in the myocardium of EAM mice and EAM mice administered linagliptin. Scale bar: 2 mm, \* $p < 0.05$ ,  $n = 6$ . Data are expressed as mean  $\pm$  SEM.

**FIGURE 2** Treatment With Linagliptin Attenuates Inflammatory Cell Infiltration in ICIM Hearts



Continued on the next page

immune response of Th17 cells through a chemotactic effect of DPP-4 (7). To examine the effects of linagliptin on the number of Th17 cells in EAM, immunostaining was performed using a ROR $\gamma$ t antibody, marker of Th17 cells. The number of Th17 cells infiltrating the myocardial tissue of EAM was markedly suppressed by linagliptin treatment (Figure 3C). We also found that DPP-4 was colocalized with ROR $\gamma$ t in the infiltrating cells of the EAM hearts (Figure 3D).

These results indicate that the increase in DPP-4 activity was significantly suppressed by linagliptin treatment in EAM hearts, possibly through suppressing the number of ROR $\gamma$ t-positive Th17 cells infiltrated to the EAM hearts.

#### DPP-4 PHYSICALLY INTERACTS WITH CATHEPSIN G, A MEMBRANE-BOUND SERINE PROTEASE, IN EAM HEARTS.

In order to elucidate how DPP-4 contributes to the progression of EAM, proteins that interact with DPP-4 in EAM myocardial tissues were explored by a TMT method using mass spectrometric analyses. Specifically, we immunoprecipitated a homogenate of Flag-DPP-4 or Flag-empty proteins with EAM myocardial tissues and labeled each immunoprecipitate with a different probe to subtract the signal of nonspecific binding substances (Figure 4A). Using this technique, we found that cathepsin G strongly interacts with DPP-4 (Figures 4B and 4C). Coimmunoprecipitation assays demonstrated that endogenous cathepsin G strongly interacted with Flag-DPP-4 *in vivo* (Figure 4D). These results suggest that DPP-4 physically interacts with cathepsin G in EAM hearts.

#### DPP-4 INCREASES CATHEPSIN G ACTIVITY IN EAM HEARTS.

The activity of cathepsin G in EAM hearts was significantly elevated; furthermore, linagliptin treatment suppressed DPP-4 activity and also cathepsin G activity in EAM hearts (Figure 5A), suggesting that the suppression of DPP-4 decreases cathepsin G activity in EAM hearts. Based on these findings, DPP-4 could play a critical role in protecting cathepsin G activity by binding with it. However, DPP-4 cannot directly regulate cathepsin G activity

because cathepsin G does not have X-proline/alanine dipeptides in its N-terminus. To resolve this conundrum, we speculated that DPP-4 inactivates cathepsin G-suppressing protease(s) containing a X-Pro/Ala peptide sequence in its/their N-terminus. *In silico* analyses revealed that SerpinA3N, a serine protease inhibitor, could be a possible candidate for such an enzyme. A previous study demonstrated that SerpinA3N inhibits activity of cathepsin G as well (17). To test this hypothesis, we examined the association between the activity of DPP-4, cathepsin G, and SerpinA3N using *in vitro* assays. The activity of cathepsin G was significantly suppressed by SerpinA3N and was restored by the presence of DPP-4 (Figure 5B). We also found that the inhibitory potential of SerpinA3N against the Granzyme B enzymatic activity was significantly stronger in the absence of DPP-4 (Figure 5C). Taken together, these results suggest that DPP-4 increases cathepsin G activity possibly through the suppression of SerpinA3N activity in EAM hearts (Figure 5D).

#### LINAGLIPTIN INCREASES SerpinA3N ACTIVITY IN EAM HEARTS.

An ELISA of myocardial lysates revealed that treatment with linagliptin does not affect the protein levels of SerpinA3N, although the amount of SerpinA3N was significantly elevated in EAM hearts (Figure 6A). We next evaluated the activity of SerpinA3N in EAM myocardial tissues by an *in vitro* Granzyme B enzymatic activity assay and found that the activity of recombinant Granzyme B was significantly suppressed by lysates of linagliptin-treated EAM myocardial tissues compared with those of untreated ones (Figure 6B). These results suggest that linagliptin promotes SerpinA3N activity in EAM hearts by inhibiting DPP-4 activity.

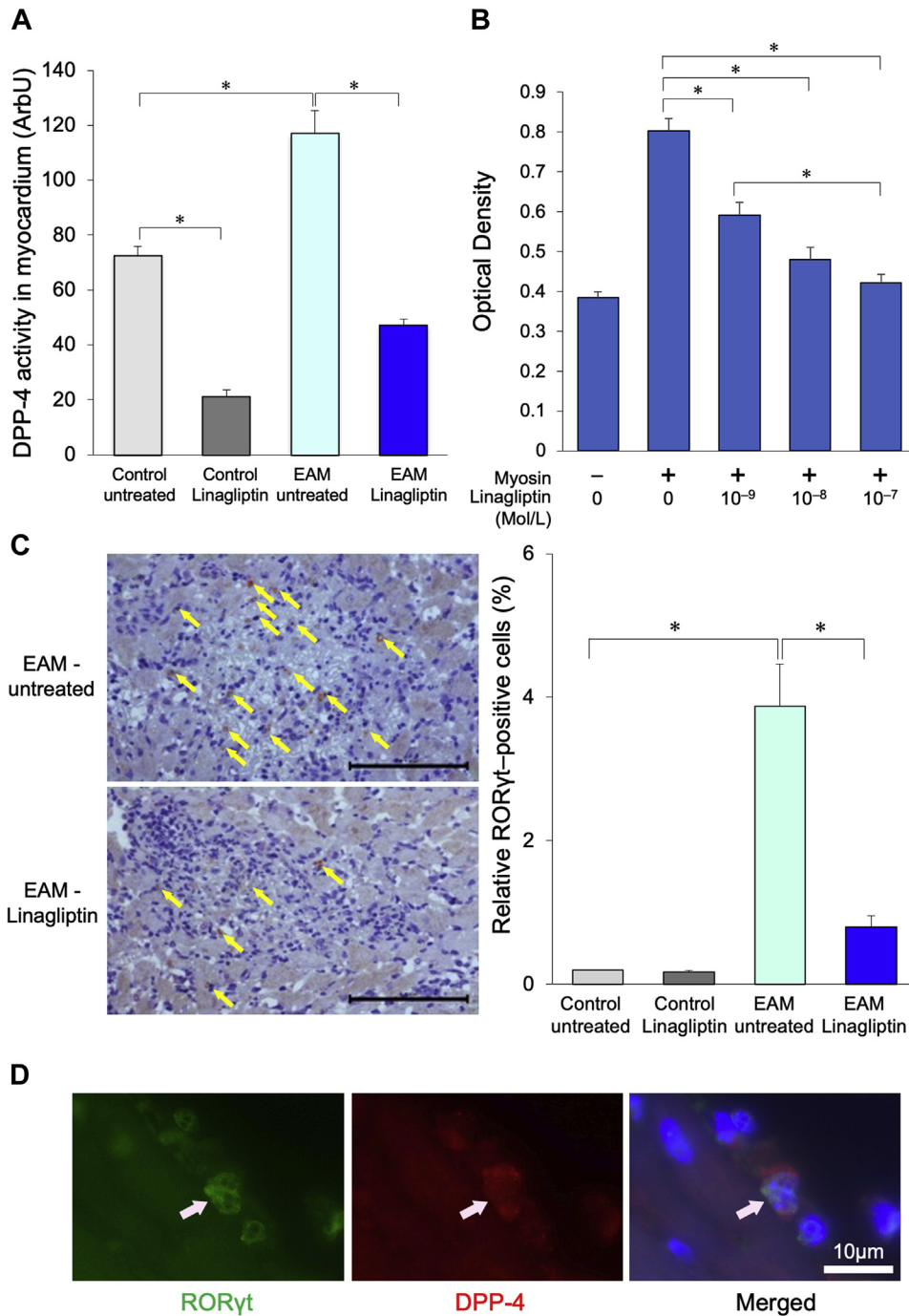
#### DPP-4 UPREGULATES ANGIOTENSIN II IN EAM HEARTS.

Previous investigations have revealed that the renin-angiotensin system plays detrimental roles in the progression of EAM (18-20). Because cathepsin G is an alternative enzyme that promotes angiotensin II production from angiotensinogen and/or

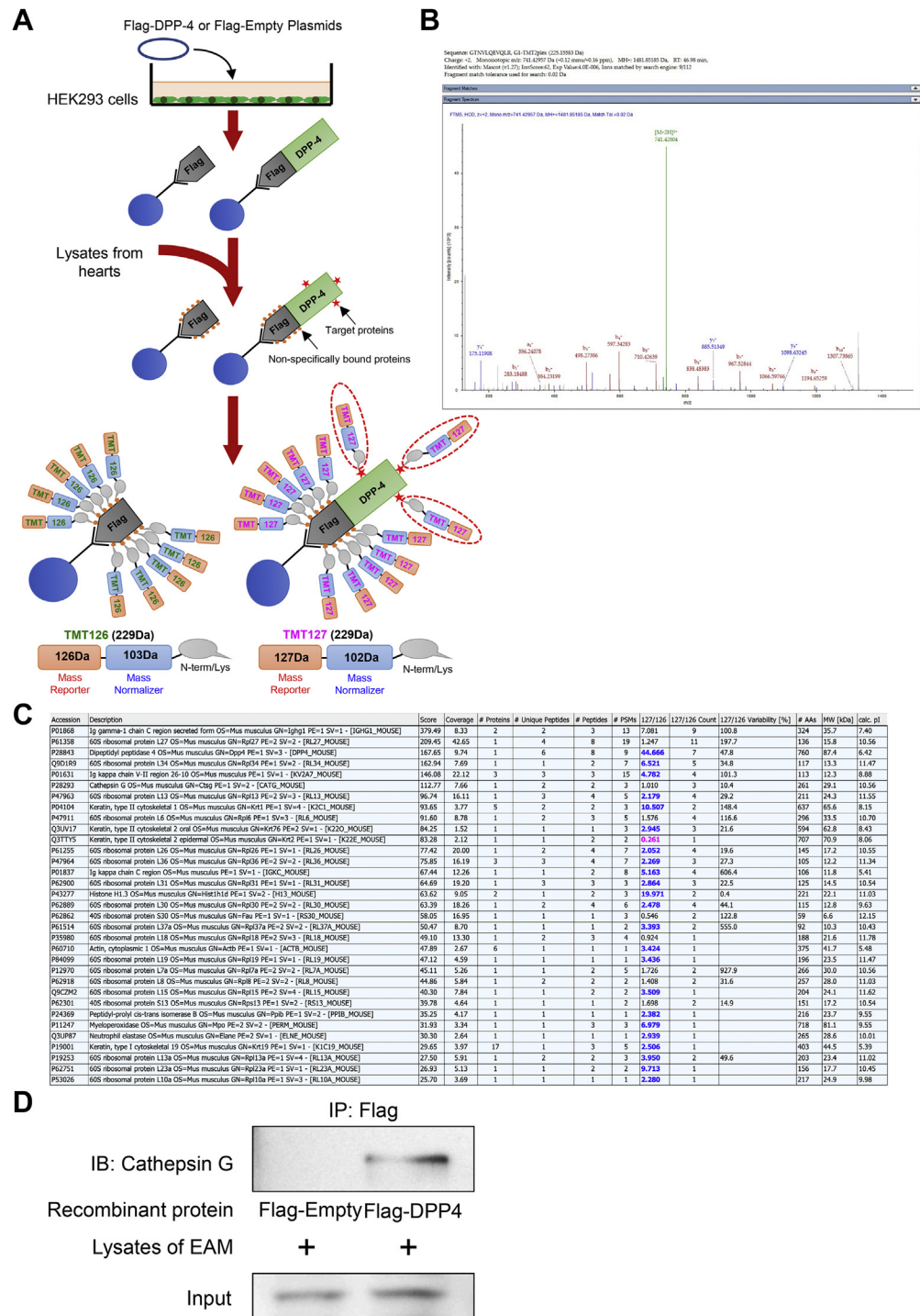
#### FIGURE 2 Continued

(A) A schematic of the experimental design for the immune checkpoint inhibitor-induced myocarditis (ICIM) model. MRL/MpJ-*Fas<sup>lpr</sup>* mice were intraperitoneally injected with both anti-PD-1 and anti-PD-L1 antibodies on days 0, 3, 7, 10, 14, 17, and 21 with or without linagliptin administration. Mice were sacrificed for analyses on day 28. (B) Representative images of inflammatory cell infiltration in the myocardium of untreated ICIM mice and ICIM mice administered linagliptin. Scale bar: 1,600  $\mu$ m (400  $\mu$ m in inset). (C) The lung weight to body weight ratio in ICIM mice and ICIM mice administered linagliptin. \* $p < 0.05$ ,  $n = 6$ . Data are expressed as mean  $\pm$  standard error of the mean (SEM). (D) Quantitative analyses of left ventricular ejection fraction in ICIM mice and ICIM mice administered linagliptin. \* $p < 0.05$ ,  $n = 6$ . Data are expressed as mean  $\pm$  SEM. (E) Quantitative analysis of the cell infiltration area in the myocardium of ICIM mice and ICIM mice administered linagliptin. Scale bar: 100  $\mu$ m, \* $p < 0.05$ ,  $n = 6$ . Data are expressed as mean  $\pm$  SEM. (F) Quantitative analysis of the fibrotic area in the myocardium of ICIM mice and ICIM mice administered linagliptin. \* $p < 0.05$ ,  $n = 6$ . Data are expressed as mean  $\pm$  SEM.

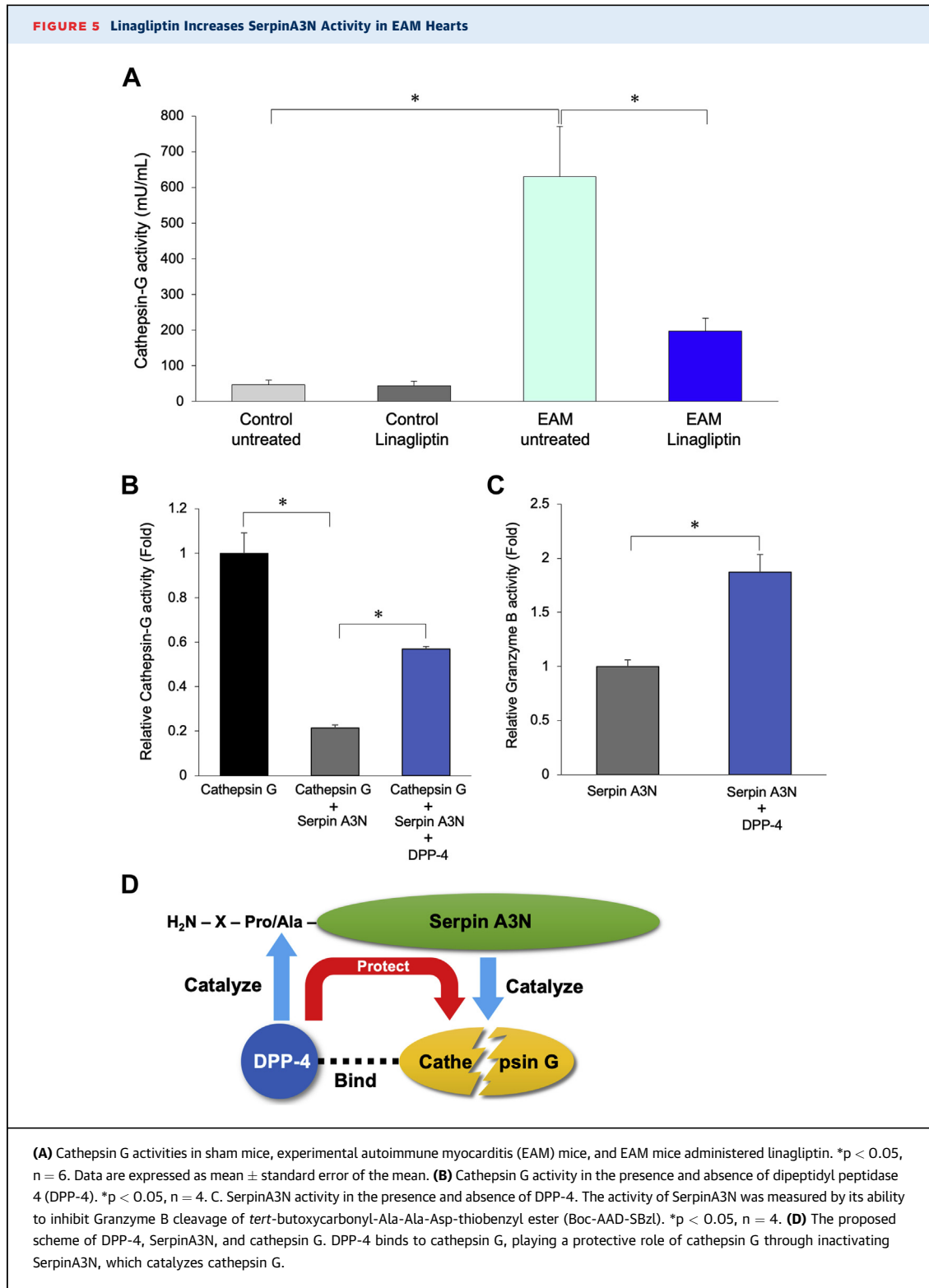
**FIGURE 3** The Increase in DPP-4 Activity Was Significantly Suppressed by Linagliptin Treatment in EAM Hearts



**(A)** The activity of dipeptidyl peptidase 4 (DPP-4) in the myocardium of sham mice, sham mice administered linagliptin, experimental autoimmune myocarditis (EAM) mice, and EAM mice administered linagliptin. \* $p < 0.05$ ,  $n = 6$ . Data are expressed as mean  $\pm$  standard error of the mean (SEM). **(B)** T-cell proliferation assays. CD4-positive T cells were isolated from splenocytes of EAM on day 18. Cells were stimulated with cardiac myosin at various concentrations of linagliptin. \* $p < 0.05$ ,  $n = 9$ . Data are expressed as mean  $\pm$  SEM. **(C)** Representative immunostaining and quantitative analysis of RAR-related orphan nuclear receptor gamma (RORγt)-positive Th17 cells in EAM mice and EAM mice administered linagliptin. **Arrows** indicate RORγt-positive Th17 cells. Scale bar: 100 μm, \* $p < 0.05$ ,  $n = 6$ . Data are expressed as mean  $\pm$  SEM. **(D)** Representative confocal immunofluorescent images of RORγt-positive Th17 cells colocalized with DPP-4 in the infiltrating cells of the EAM hearts.

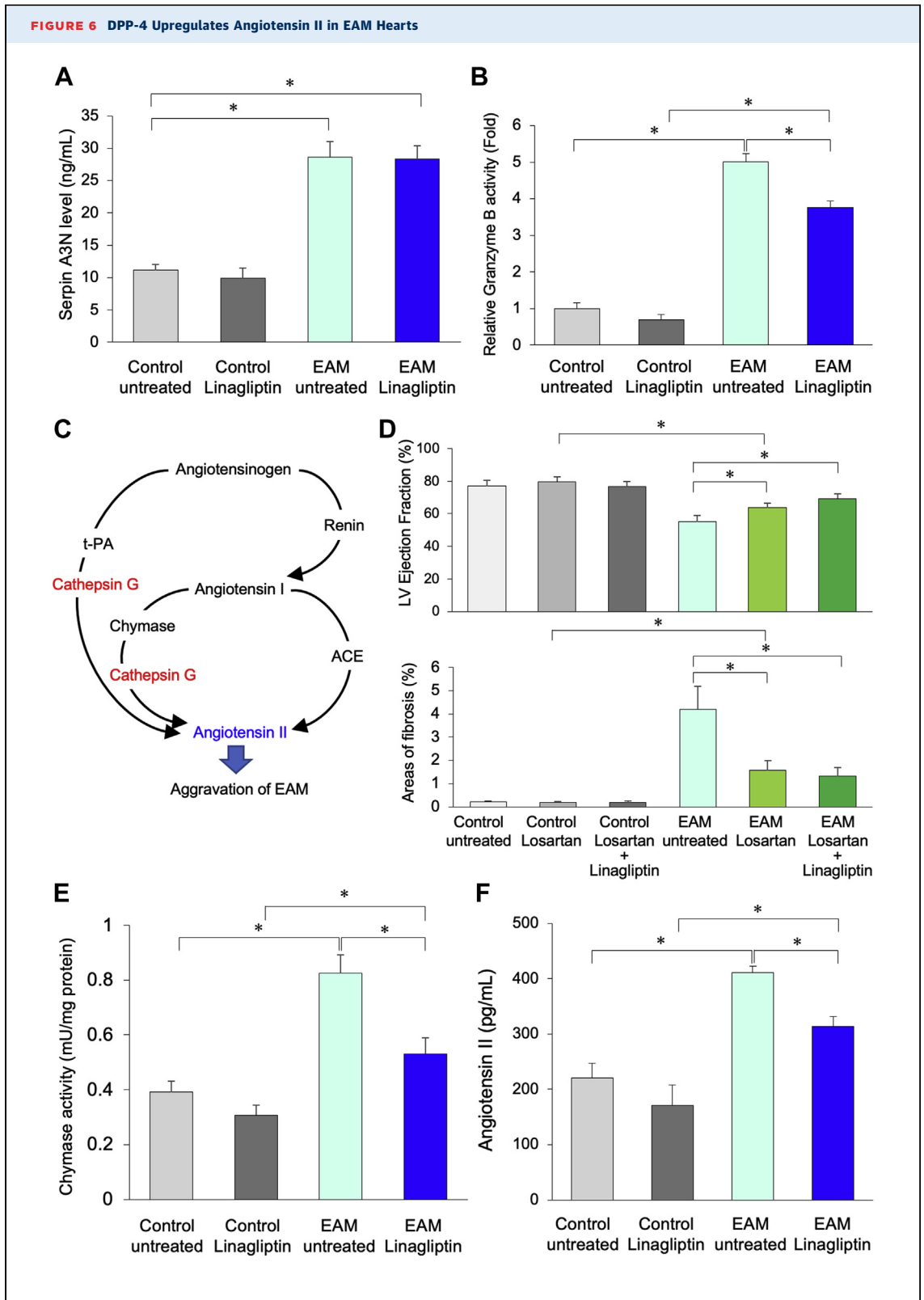
**FIGURE 4 DPP-4 Physically Interacts With Cathepsin G, a Membrane-Bound Serine Protease, in EAM Hearts**

**(A)** Comprehensive analysis for detecting novel proteins that interact with dipeptidyl peptidase 4 (DPP-4) using a tandem mass tag method on mass spectrometric analyses. Flag-DPP-4 or Flag-empty proteins conjugated with magnetic beads via an anti-Flag antibody were immunoprecipitated with lysates from experimental autoimmune myocarditis (EAM) myocardial tissues. Each immunoprecipitate was labeled with a different probe to subtract the signal of nonspecific binding substances. **(B)** Liquid chromatography tandem mass spectrometry was performed on these samples, and data were analyzed to detect the proteins that bind most to DPP-4; **(C)** peptides were identified by comparing them against the *Mus musculus* protein database. **(D)** Immunoprecipitation analyses of recombinant proteins, Flag-empty, and Flag-tagged DPP-4.



angiotensin I (Figure 6C), DPP-4-mediated cathepsin G activation should aggravate EAM by elevating the amount of angiotensin II in myocardial tissues. Consistent with this hypothesis, left ventricular

systolic function was significantly higher in EAM hearts treated with losartan, an angiotensin II receptor type 1 antagonist, than in untreated ones after 21 days of EAM induction and cardiac fibrosis after



EAM induction was significantly decreased by treatment with losartan (Figure 6D). Because it has been shown that SerpinA3N also catalyzes chymase (21), we examined the effect of linagliptin on the chymase activity in EAM hearts and found that the activity of chymase in EAM hearts was significantly elevated and linagliptin treatment markedly suppressed the chymase activity (Figure 6E). Expression levels of angiotensin II were significantly elevated in EAM hearts; conversely, expression levels were suppressed by linagliptin treatment (Figure 6F).

These results suggest that DPP-4 upregulates angiotensin II in EAM hearts, possibly through the enhancement of cathepsin G activity.

**LINAGLIPTIN SUPPRESSES OXIDATIVE STRESS IN EAM HEARTS.** To examine whether linagliptin, a xanthine-based DPP-4 inhibitor, could attenuate oxidative stress in EAM hearts, levels of oxidative stress in the myocardium were determined. The amount of hydrogen peroxide (H<sub>2</sub>O<sub>2</sub>) in EAM hearts was significantly elevated compared with those in the control; moreover, H<sub>2</sub>O<sub>2</sub> amounts in EAM hearts were significantly suppressed by linagliptin treatment (Figure 7A). Similarly, the number of 8-OHdG-positive cells in the nuclei, a marker of oxidative stress in cellular DNA, was significantly higher in EAM hearts than those in control, and the number of 8-OHdG-positive cells was significantly decreased by linagliptin treatment (Figure 7B). These results suggest that the beneficial effects of linagliptin on EAM hearts are partially mediated through the inhibition of oxidative stress.

## DISCUSSION

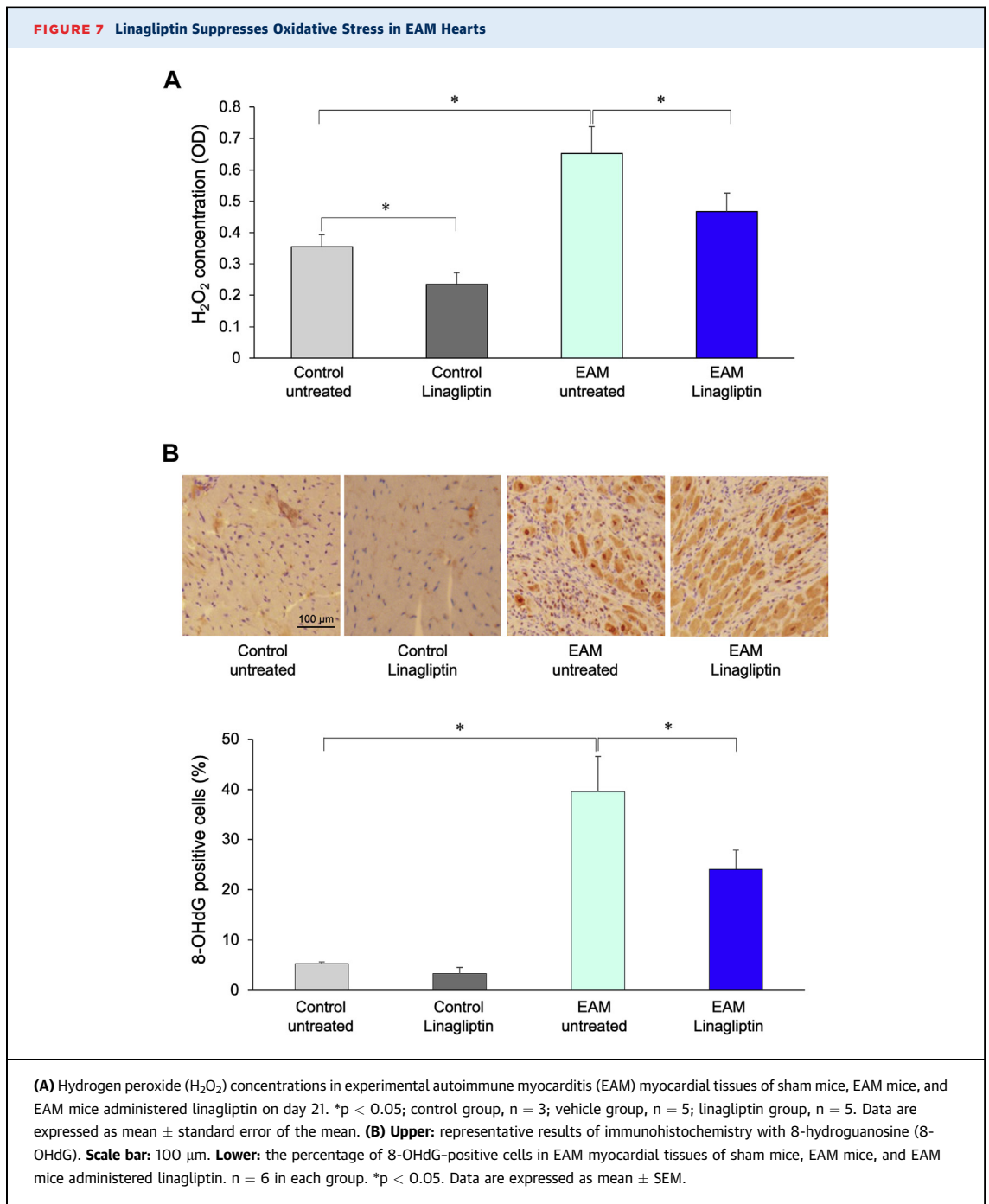
Previous reports have shown that the administration of linagliptin attenuates myocardial inflammation by suppressing cardiac fibrosis, abrogating oxidative stress, and reducing inflammatory cytokine gene expression in EAM mice (12,22). In the present study,

we revealed a novel mechanism to attenuate autoimmune myocarditis by linagliptin administration. We also observed that the administration of linagliptin alleviates pathological phenotypes of ICIM hearts. Furthermore, we determined that DPP-4 physically interacts with cathepsin G, thereby enhancing intramyocardial cathepsin G activity by suppressing SerpinA3N. We also found that linagliptin reduces the amount of angiotensin II, a substrate of cathepsin G, which could be responsible for the aggravation of EAM.

Unbiased comprehensive proteomic analyses with validation assays revealed an association between DPP-4 and cathepsin G. As stated earlier, we identified that DPP-4 protects cathepsin G by inhibiting SerpinA3N activity using both in silico and in vitro analyses. Increasing lines of evidence suggest that cathepsin G, a serine protease that principally locates in azurophilic granules of myeloid cells, plays important roles in the development of inflammation by promoting immune cell migration and activating chemokines (23,24). Additionally, it is well-known that cathepsin G participates in the pathogenesis of various autoimmune disorders, such as rheumatoid arthritis, systemic lupus erythematosus, and autoimmune diabetes (25-27). Consistently, we demonstrated that cathepsin G activity in EAM hearts was significantly elevated and that the administration of linagliptin attenuated immune cell migration and cathepsin G activity in the myocardium. To explore in more detail how cathepsin G is associated with the pathogenesis of EAM, we focused on the role of angiotensin II, one of the major substrates of cathepsin G, in the progression of EAM. A growing body of evidence suggests that activation of the renin-angiotensin system causes an increase in the release of proinflammatory cytokines/chemokines and the production of reactive oxygen species, thereby leading to the inflammation and development of autoimmune diseases. Indeed, previous

### FIGURE 6 Continued

(A) Protein levels of SerpinA3N in experimental autoimmune myocarditis (EAM) myocardial tissues of sham mice, EAM mice, and EAM mice administered linagliptin. \*p < 0.05, n = 6. Data are expressed as mean ± standard error of the mean (SEM). (B) SerpinA3N activity in EAM myocardial tissues of sham mice, EAM mice, and EAM mice administered linagliptin. \*p < 0.05, n = 6. Data are expressed as mean ± SEM. (C) The mechanism of cathepsin G-related angiotensin II generating system. Angiotensin II is generated from a renin-angiotensin system and multiple enzymes such as cathepsin G. Cathepsin G can convert angiotensin I to angiotensin II and also can directly convert angiotensinogen to angiotensin II. (D) Upper: quantitative analyses of left ventricular ejection fraction in EAM mice with or without administration with linagliptin and/or losartan. \*p < 0.05, n = 6. Data are expressed as mean ± SEM. Lower: quantitative analysis of the fibrotic area in the myocardium of EAM mice with or without the administration of linagliptin and/or losartan. \*p < 0.05, n = 6. Data are expressed as mean ± SEM. (E) Chymase activity in EAM myocardial tissues of sham mice, EAM mice, and EAM mice administered linagliptin. \*p < 0.05, n = 6. Data are expressed as mean ± SEM. (F) The amount of angiotensin II in EAM myocardial tissues of sham mice, EAM mice, and EAM mice administered linagliptin. \*p < 0.05, n = 6. Data are expressed as mean ± SEM.



studies have shown that the suppression of the renin-angiotensin system by treatment with an angiotensin-converting enzyme inhibitor, angiotensin II receptor type 1 blocker, and renin inhibitor effectively alleviates cardiac dysfunction caused by EAM (18-20). Thus, the suppression of cathepsin G, which catalyzes angiotensin II production from angiotensinogen and/or angiotensin I, should be an effective target for the suppression of EAM activity.

Consistently, we demonstrate that the suppression of DPP-4 by linagliptin effectively suppressed angiotensin II levels in EAM hearts. Taken together, our current data suggest that the suppression of cathepsin G activity via DPP-4 inhibition could be a reasonable therapeutic strategy for EAM hearts.

A vast number of previous preclinical studies demonstrated that DPP-4 inhibitors play beneficial roles in the progression of cardiovascular diseases,

including heart failure. For example, the administration of DPP-4 inhibitors improves diastolic failure in diabetic rats, possibly by maintaining blood levels of chemokine stromal cell-derived factor 1, which is a DPP-4 substrate (28). The administration of DPP-4 inhibitors to a post-cardiac infarction heart failure model showed significant improvement in cardiac function through the activation of protein kinase A and the promotion of angiogenesis in the myocardium (29). Thus, DPP-4 inhibitors are expected to be potent therapeutic agents against heart failure. On the other hand, 4 cardiovascular outcome trials have been performed (the EXAMINE [Examination of Cardiovascular Outcomes With Alogliptin versus Standard of Care] trial [30], the SAVOR-TIMI 53 [Saxagliptin Assessment of Vascular Outcomes Recorded in Patients with Diabetes Mellitus-Thrombolysis in Myocardial Infarction 53] trial with saxagliptin [31], the TECOS [Trial Evaluating Cardiovascular Outcomes with Sitagliptin] trial [32], and the CARMELINA [Cardiovascular and Renal Microvascular Outcome Study with Linagliptin] trial with linagliptin [33]), but none of them demonstrated the utility of DPP-4 inhibitors on overall heart failure despite our expectations. Rather, the SAVOR-TIMI 53 trial showed that hospitalizations due to heart failure in diabetic patients who received saxagliptin increased by 27% compared with patients who received the placebo. Thus, there is a discrepancy between the effects of DPP-4 inhibitors in pre-clinical trials and those in clinical trials. However, there is still the possibility that DPP-4 inhibitors may be useful for the treatment of heart failure when a clinical state is appropriately selected, such as inflammation-based heart failure. To verify such hypothesis, further clinical investigations need to be conducted.

It has been shown that linagliptin is a unique DPP-4 inhibitor that may exert antioxidant effects because it has a xanthine-based molecular structure (34,35). Oxidative stress plays an important role in the progression of EAM (36). Our current study demonstrated that the levels of H<sub>2</sub>O<sub>2</sub> in the myocardium and the number of 8-OHdG-positive cells decreased after linagliptin treatment. This suggests a beneficial effect of linagliptin on EAM that may be mediated by suppressing oxidative stress, a quality that no other DPP-4 inhibitor may have.

In summary, we confirmed that the inhibition of DPP-4 by linagliptin is an effective strategy to relieve the disease status of EAM. We also described a novel mechanism of immunosuppression that is different from the conventionally known mechanisms. Although the results of existing clinical trials have not

shown the beneficial effects of DPP-4 inhibitors in heart failure, the administration of DPP-4 inhibitors has a potential for clinical applications as a new therapeutic strategy for the treatment of inflammation-mediated heart diseases.

**ACKNOWLEDGMENTS** We would like to thank Ms. Noriko Tamura for excellent technical assistance. We also thank Boehringer Ingelheim for providing linagliptin.

#### FUNDING SUPPORT AND AUTHOR DISCLOSURES

This work was supported in part by a grant from Boehringer Ingelheim and JSPS KAKENHI Grant-in-Aid for Scientific Research (C) (17K09570 to Dr. Maejima). Dr. Maejima has received speaker honoraria from AstraZeneca, Bayer, and Boehringer Ingelheim; and has received research support from AstraZeneca, Boehringer Ingelheim, Bayer, Bristol-Myers Squibb, Chugai Pharmaceuticals, Eli Lilly, Merck Sharpe & Dohme, Novartis Pharma, and Taisho-Tomiyama Pharmaceuticals. All other authors have reported that they have no relationships relevant to the contents of this paper to disclose.

**ADDRESS FOR CORRESPONDENCE:** Dr. Yasuhiro Maejima, Department of Cardiovascular Medicine, Tokyo Medical and Dental University, 1-5-45 Yushima, Bunkyo-ku, Tokyo 113-8519, Japan. E-mail: [ymaeji.cvm@tmd.ac.jp](mailto:ymaeji.cvm@tmd.ac.jp).

#### PERSPECTIVES

**COMPETENCY IN MEDICAL KNOWLEDGE:** Despite the fact that autoimmune myocarditis is a rare cardiovascular disease, there is a compelling need for establishing effective therapy because of its serious clinical manifestations, including heart failure and sudden death. In addition, autoimmune myocarditis has received a lot of attention in recent years as a serious side effect of immune checkpoint inhibitors. We assessed the impact of linagliptin, a xanthine-based dipeptidyl peptidase 4 inhibitor, on both EAM and ICIM and explored the underlying molecular mechanism of how DPP-4 aggravates autoimmune myocarditis.

**TRANSLATIONAL OUTLOOK:** Our study demonstrated that linagliptin reduced inflammatory cell infiltration and ameliorated cardiac fibrosis, which normalized left ventricular systolic function and alleviated lung congestion in autoimmune myocarditis. Importantly, these beneficial effects of linagliptin are mediated through suppressing DPP-4, which enhances the activity of cathepsin G, a binding partner of DPP-4, by inhibiting SerpinA3N activity as well as its antioxidant effect. These findings suggest that DPP-4 inhibitors could be useful for the treatment of inflammation-based heart diseases, whereas 4 large trials have demonstrated that DPP-4 inhibitors had no beneficial effects for cardiovascular outcome in patients with type 2 diabetes.

## REFERENCES

1. Maisch B, Pankuweit S. Current treatment options in (peri)myocarditis and inflammatory cardiomyopathy. *Herz* 2012;37:644-56.
2. Feldman AM, McNamara D. Myocarditis. *N Engl J Med* 2000;343:1388-98.
3. Johnson DB, Balko JM, Compton ML, et al. Fulminant myocarditis with combination immune checkpoint blockade. *N Engl J Med* 2016;375:1749-55.
4. Salem JE, Manouchehri A, Moey M, et al. Cardiovascular toxicities associated with immune checkpoint inhibitors: an observational, retrospective, pharmacovigilance study. *Lancet Oncol* 2018;19:1579-89.
5. Proost P, Struyf S, Schols D, et al. Truncation of macrophage-derived chemokine by cd26/dipeptidyl-peptidase iv beyond its predicted cleavage site affects chemotactic activity and cc chemokine receptor 4 interaction. *J Biol Chem* 1999;274:3988-93.
6. Zhong J, Maiseyeu A, Davis SN, Rajagopalan S. Dpp4 in cardiometabolic disease: Recent insights from the laboratory and clinical trials of dpp4 inhibition. *Circ Res* 2015;116:1491-504.
7. Bengsch B, Seigel B, Flecken T, Wolanski J, Blum HE, Thimme R. Human th17 cells express high levels of enzymatically active dipeptidylpeptidase iv (cd26). *J Immunol* 2012;188:5438-47.
8. Zhong J, Rao X, Deilulis J, et al. A potential role for dendritic cell/macrophage-expressing dpp4 in obesity-induced visceral inflammation. *Diabetes* 2013;62:149-57.
9. Fuchs H, Binder R, Greischel A. Tissue distribution of the novel dpp-4 inhibitor bi 1356 is dominated by saturable binding to its target in rats. *Biopharm Drug Dispos* 2009;30:229-40.
10. Darsalia V, Ortsater H, Olverling A, et al. The dpp-4 inhibitor linagliptin counteracts stroke in the normal and diabetic mouse brain: a comparison with glimepiride. *Diabetes* 2013;62:1289-96.
11. Kanasaki K, Shi S, Kanasaki M, et al. Linagliptin-mediated dpp-4 inhibition ameliorates kidney fibrosis in streptozotocin-induced diabetic mice by inhibiting endothelial-to-mesenchymal transition in a therapeutic regimen. *Diabetes* 2014;63:2120-31.
12. Hirakawa H, Zempo H, Ogawa M, et al. A dpp-4 inhibitor suppresses fibrosis and inflammation on experimental autoimmune myocarditis in mice. *PLoS One* 2015;10:e0119360.
13. Ito Y, Maejima Y, Tamura N, et al. Synergistic effects of hmg-coa reductase inhibitor and angiotensin ii receptor blocker on load-induced heart failure. *FEBS Open Bio* 2018;8:799-816.
14. Ratcliffe NR, Hutchins J, Barry B, Hickey WF. Chronic myocarditis induced by t cells reactive to a single cardiac myosin peptide: persistent inflammation, cardiac dilatation, myocardial scarring and continuous myocyte apoptosis. *J Autoimmun* 2000;15:359-67.
15. Kanemitsu H, Takai S, Tsuneyoshi H, et al. Chymase inhibition prevents cardiac fibrosis and dysfunction after myocardial infarction in rats. *Hypertens Res* 2006;29:57-64.
16. Kodama M, Matsumoto Y, Fujiwara M. In vivo lymphocyte-mediated myocardial injuries demonstrated by adoptive transfer of experimental autoimmune myocarditis. *Circulation* 1992;85:1918-26.
17. Horvath AJ, Irving JA, Rossjohn J, et al. The murine orthologue of human antichymotrypsin: a structural paradigm for clade a3 serpins. *J Biol Chem* 2005;280:43168-78.
18. Godsel LM, Leon JS, Wang K, Fornek JL, Molteni A, Engman DM. Captopril prevents experimental autoimmune myocarditis. *J Immunol* 2003;171:346-52.
19. Liu X, Zhu X, Wang A, Fan H, Yuan H. Effects of angiotensin-ii receptor blockers on experimental autoimmune myocarditis. *Int J Cardiol* 2009;137:282-8.
20. Takamura C, Suzuki J, Ogawa M, et al. Suppression of murine autoimmune myocarditis achieved with direct renin inhibition. *J Cardiol* 2016;68:253-60.
21. Wagsater D, Johansson D, Fontaine V, et al. Serine protease inhibitor a3 in atherosclerosis and aneurysm disease. *Int J Mol Med* 2012;30:288-94.
22. Aroor AR, Habibi J, Kandikattu HK, et al. Dipeptidyl peptidase-4 (dpp-4) inhibition with linagliptin reduces western diet-induced myocardial traf3ip2 expression, inflammation and fibrosis in female mice. *Cardiovasc Diabetol* 2017;16:61.
23. Richter R, Bistrrian R, Escher S, et al. Quantum proteolytic activation of chemokine ccl15 by neutrophil granulocytes modulates mononuclear cell adhesiveness. *J Immunol* 2005;175:1599-608.
24. Nufer O, Corbett M, Walz A. Amino-terminal processing of chemokine ena-78 regulates biological activity. *Biochemistry* 1999;38:636-42.
25. Miyata J, Tani K, Sato K, et al. Cathepsin g: the significance in rheumatoid arthritis as a monocyte chemoattractant. *Rheumatol Int* 2007;27:375-82.
26. Tamiya H, Tani K, Miyata J, et al. Defensins and cathepsin g-anca in systemic lupus erythematosus. *Rheumatol Int* 2006;27:147-52.
27. Zou F, Lai X, Li J, Lei S, Hu L. Downregulation of cathepsin g reduces the activation of cd4+ t cells in murine autoimmune diabetes. *Am J Transl Res* 2017;9:5127-37.
28. Shigeta T, Aoyama M, Bando YK, et al. Dipeptidyl peptidase-4 modulates left ventricular dysfunction in chronic heart failure via angiogenesis-dependent and -independent actions. *Circulation* 2012;126:1838-51.
29. Birnbaum Y, Castillo AC, Qian J, et al. Phosphodiesterase III inhibition increases camp levels and augments the infarct size limiting effect of a dpp-4 inhibitor in mice with type-2 diabetes mellitus. *Cardiovasc Drugs Ther* 2012;26:445-56.
30. White WB, Cannon CP, Heller SR, et al. Alogliptin after acute coronary syndrome in patients with type 2 diabetes. *N Engl J Med* 2013;369:1327-35.
31. Scirica BM, Bhatt DL, Braunwald E, et al. Saxagliptin and cardiovascular outcomes in patients with type 2 diabetes mellitus. *N Engl J Med* 2013;369:1317-26.
32. Green JB, Bethel MA, Armstrong PW, et al. Effect of sitagliptin on cardiovascular outcomes in type 2 diabetes. *N Engl J Med* 2015;373:232-42.
33. Rosenstock J, Perkovic V, Johansen OE, et al. Effect of linagliptin vs placebo on major cardiovascular events in adults with type 2 diabetes and high cardiovascular and renal risk: the Carmelina randomized clinical trial. *JAMA* 2019;321:69-79.
34. Ghatak SB, Patel DS, Shanker N, Srivastava A, Deshpande SS, Panchal SJ. Linagliptin: a novel xanthine-based dipeptidyl peptidase-4 inhibitor for treatment of type ii diabetes mellitus. *Curr Diabetes Rev* 2011;7:325-35.
35. Kroller-Schon S, Knorr M, Hausding M, et al. Glucose-independent improvement of vascular dysfunction in experimental sepsis by dipeptidyl-peptidase 4 inhibition. *Cardiovasc Res* 2012;96:140-9.
36. Okabe TA, Kishimoto C, Hattori M, Nimata M, Shioji K, Kita T. Cardioprotective effects of 3-methyl-1-phenyl-2-pyrazolin-5-one (mci-186), a novel free radical scavenger, on acute autoimmune myocarditis in rats. *Exp Clin Cardiol* 2004;9:177-80.

**KEY WORDS** autoimmune myocarditis, dipeptidyl peptidase 4, heart failure, inflammation